Supporting Information for "Solid-State Synthesis of Efficient Supported Iridium Catalysts for the Acidic Oxygen Evolution Reaction"

*Greta Giarola, Mathias Meidahl Hommelgaard, Fabian Luca Buchauer, María Paula Salinas Quezada, Christodoulos Chatzichristodoulou, Heine Anton Hansen, Yang Hu**

Department of Energy Conversion and Storage, Technical University of Denmark, Fysikvej, 2800, Kgs. Lyngby, Denmark

EXPERIMENTAL

Materials

Iridium(IV) oxide (IrO_2, Premion®, 99.99% metals basis, Ir 84.5% min) from Alfa Aesar (now rebranded with Thermo Fisher Scientific) was used as the benchmark catalyst.

Synthesis details:

Synthesis of Nb–TiO_2 support. $Nb_{0.1}Ti_{0.9}O_2$ was synthesized via a sol-gel method. Stoichiometric amounts of titanium butoxide (97 %), niobium ethoxide (99.95 %), citric acid, and EDTA were mixed in ethanol at a cation:citric acid:EDTA molar ratio of 1:1:1.5. The resulting solution was heated at 120 °C for 4 h until a viscous gel formed. The gel was then transferred to an alumina crucible and heat-treated at 450 °C for 5 h in air. The obtained powder was subsequently crushed and sintered at 600 °C for 3 h in air.

Synthesis of Ir/Nb–TiO_2. To prepare Ir/Nb–TiO_2, 100 mg of $IrCl_3 \cdot xH_2O$ (50 wt%, Sigma-Aldrich), 50 mg of Nb–TiO_2, and 215 mg of cyanamide (CN_2H_2, 99%, Sigma-Aldrich) were mixed and ground in a mortar under ambient conditions without any solvent. The resulting mixture was transferred to a quartz boat and introduced into a tube furnace, which was evacuated and purged with Ar to remove the air. The furnace was first heated from room temperature to 600 °C at the rate of 15 °C min^{-1} under a flow of Ar (100 mL min^{-1}) and maintained at this temperature for 1 h. Subsequently, the gas flow was switched to 12% H_2/Ar, and the temperature was increased to 650 °C at a rate of 10 °C min^{-1}. The sample was held under these conditions for 1 h and then cooled down to room temperature at the rate of 25 °C min^{-1}.

Physical and chemical characterizations:

SEM-EDS: Scanning electron microscopy with energy-dispersive X-ray spectroscopy (SEM-EDS) was conducted using an AFEG 250 Analytical ESEM (FEI Quanta FEG 250) equipped with an Oxford Instruments 50 mm^2 X-Max silicon drift detector (MnKα resolution at 124 eV). EDS data acquisition and analysis were performed using Oxford Instruments Aztec software. Commercial IrO_2 with known Ir content of 84.5% was used as an external reference for calibration.

XRD: Powder X-ray diffraction (XRD) measurements were performed with a MiniFlex 600 X-ray diffractometer (Rigaku) using a Cu Kα (λ = 1.5418 Å) radiation source. Measurements were performed in the 2θ range of 5–100° with a step size of 0.02° and a scan speed of 2.0° min^{-1}.

In-situ XRD for studying the catalyst synthesis process: An automated multipurpose X-ray diffractometer (Rigaku SmartLab, Cu Kα radiation, λ = 1.5418 Å, Bragg–Brentano geometry) equipped with an HTK 1200N non-ambient chamber was used for the experiments. The sample—an intermediate collected after step 1 of the synthesis—was loaded into a quartz capillary (inner diameter 0.9 mm, wall thickness 0.1 mm), through which a flow of 5% H_2 in N_2 at 20 mL min^{-1} was maintained during the heat treatment. The sample was heated to 650 °C at 20 °C min^{-1} and held at 650 °C for 1 hour. XRD data acquisition began once the sample temperature reached 650 °C.

In-situ XRD for studying the catalyst stability during AST: In-situ XRD measurements were performed on a Rigaku Smartlab diffractometer equipped with a D/teX Ultra 250 detector, using a Cu Kα radiation (λ = 1.5418 Å) in Bragg-Brentano geometry. The instrument was operated at 45kV and 200 mA. The XRD patterns collected during the AST measurements were recorded in the 2θ range of 30–90°, with a step size of 0.05° and a scan speed of 83° min^{-1}.

TEM: Transmission electron microscopy (TEM) was performed using a FEI Tecnai 20 microscope operating at an acceleration voltage of 200 kV with a LaB_6 thermionic electron source. Images were acquired using a TVIPS XF416 CMOS camera (4096×4096 pixels). Particle size analysis was performed using ImageJ software.

STEM: High-angle annular dark-field scanning TEM (HAADF-STEM) tests were conducted at 300 kV using an Spectra Ultra STEM (Thermo Fisher Scientific) equipped with a spherical aberration corrector.**XPS:** X-ray photoelectron spectroscopy (XPS) was measured using a Thermo Fisher Scientific Nexsa under high vacuum (<10-8) with a monochromated Al Kα radiation source at 1486.6eV. All XPS spectra were corrected for the work function of the spectrometer using an ion-etched gold foil (Au 4f7/2 = 84.0 eV).

Conductivity measurements: Powder conductivity was determined by compressing the sample in a copper holder (area = 0.196 cm^2) at applied torques of 10, 16, 20.5, 25, 31, and 34 cNm. For each applied force, the resistance and powder thickness were measured. The intrinsic resistance (R) and thickness (l) of the powder layer were obtained by subtracting the values from corresponding blank measurements performed without powder. The resistance was extracted from the slope of linear sweep voltammograms (LSVs). Finally, the resistivity was calculated using $\rho = R\frac{A}{l}$, from which the conductivity was derived.

ICP-MS: Liquid sample analysis was performed via inductively coupled plasma mass spectrometry (ICP-MS) to quantify dissolved Ir species. Samples were prepared by acidification with 65% HNO_3 to reach a final concentration of 2%. Measurements tracked the ^{193}Ir isotope using a no-gas mode. Analytical reliability was ensured by analyzing each injection three times to calculate the relative standard deviation (RSD), and the quantification limit was established at 0.5 µg/L.

Electrochemical tests:

Electrochemical measurements were conducted using a Biologic VSP multichannel potentiostat at 22°C. The electrolyte was a 0.1 M $HClO_4$ solution, prepared by diluting high-purity $HClO_4$ (65-71%, Normatom, VWR) with Milli-Q water. The catalyst ink was prepared by dispersing the catalyst in isopropanol (98%, VWR) with a 5wt% solution of Nafion as the binder (catalyst:Nafion mass ratio of 10:1). The ink was sonicated to yield a uniform dispersion. To prepare the thin catalyst film, 50 µL of the ink were sprayed onto a custom-made rotating disk electrode (RDE, 0.196 cm^2) composed of gold and PEEK. A standard three-electrode cell was used for all measurements, consisting of the RDE as the working electrode, a platinum wire as the counter electrode and a self-prepared reversible hydrogen electrode (RHE) as the reference electrode. The reference and counter electrodes were separated from the working electrode compartment using porous glass frits. All glassware was cleaned in concentrated H_2SO_4 overnight and boiled in Milli-Q water at least three times before use. Prior to the tests the electrolyte was saturated with high-purity Ar. To conduct activation, the catalyst was cycled between 0.025 V and 1.4 V at 100 mV s^{-1} for 70 cycles, until a stable cyclic voltammogram (CV) was obtained. Catalytic activity was measured by recording 3 CVs between 1.2 V and 1.6 V at 20 mV s^{-1}. The accelerated stress test (AST) protocol consisted of cycling between 1.2 V and 1.6 V at 100 mV s^{-1} for 1800 cycles. After the AST, the electrolyte was replaced and saturated again with Ar, and the activity of the catalyst was measured again. The uncompensated electrolyte resistance (R_u) was measured with electrochemical impedance spectroscopy (EIS) at open circuit potential by applying an AC signal with 10 mV amplitude over the frequency range from 200 kHz to 0.1 Hz.

To determine the catalyst loading of the sprayed films, a calibration was carried out using drop-casted films. The ink for drop casting was prepared similarly to the spray ink but with a solvent mixture of isopropanol and milli-Q water (3:1 water to isopropanol volume ratio) to account for the different tension angles of the solvents on the gold surface. 5 µL of the ink was drop cast on the RDE, corresponding to a loading of 15 μg_{Ir} cm^{-2}. The CV after activation was used for calibration: the area of the non-faradaic region between 0.4 V and 0.6 V was measured and attributed to the loading of 15 μg_{Ir} cm^{-2}.

SUPPLEMENTARY FIGURES

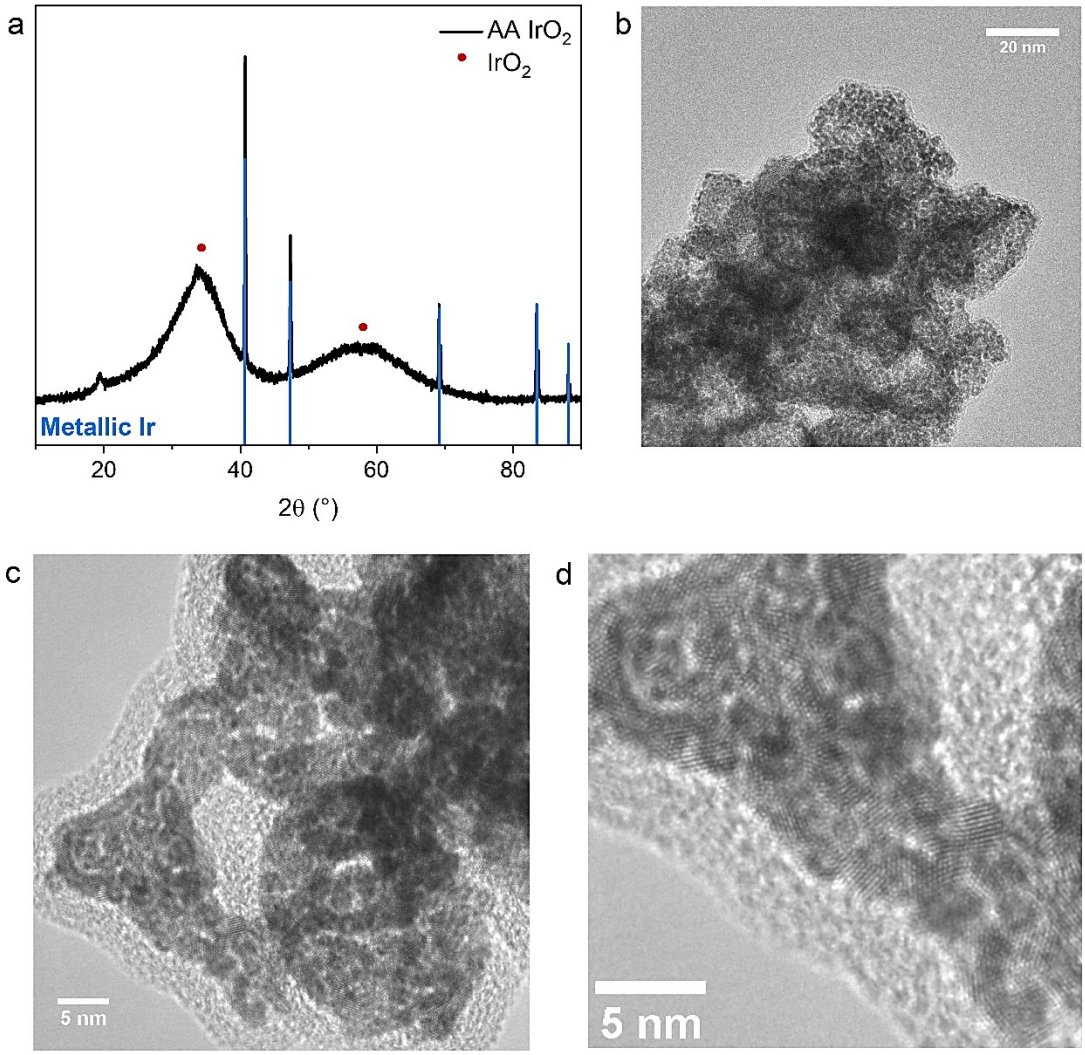

Figure S1. (a) XRD pattern of AA IrO_2. The blue vertical lines represent the reference pattern for metallic Ir (PDF 65-9327). According to Rietveld refinement of the XRD data reported in literature, the content of metallic Ir is below 2 wt%.[1,2] (b,c,d) TEM images of AA IrO_2, which show ordered crystalline structures of the ultra-small (about 1.6 nm) IrO_2 particles.

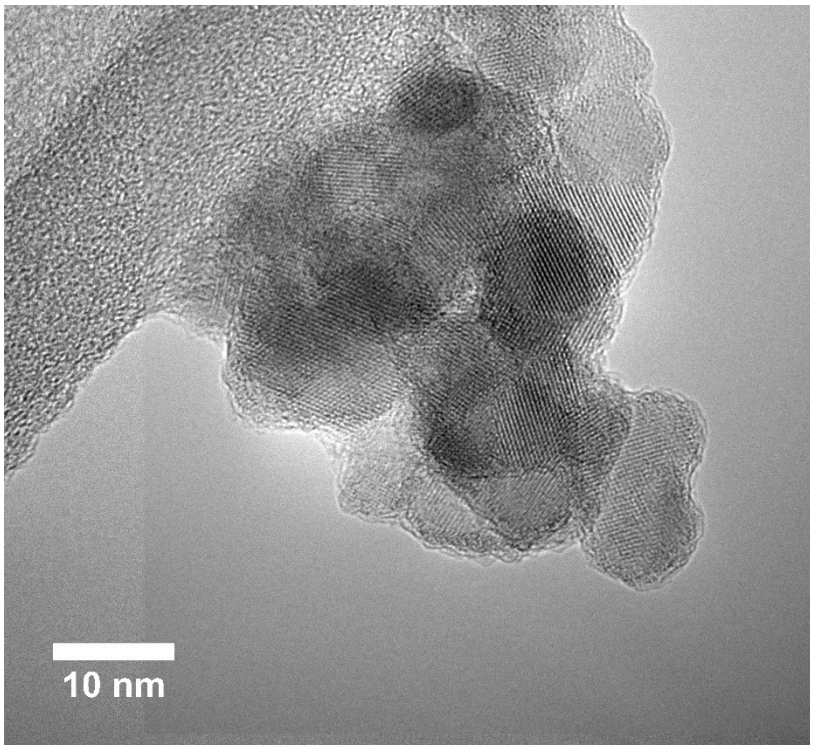

Figure S2. TEM image of Nb-TiO_2 support.

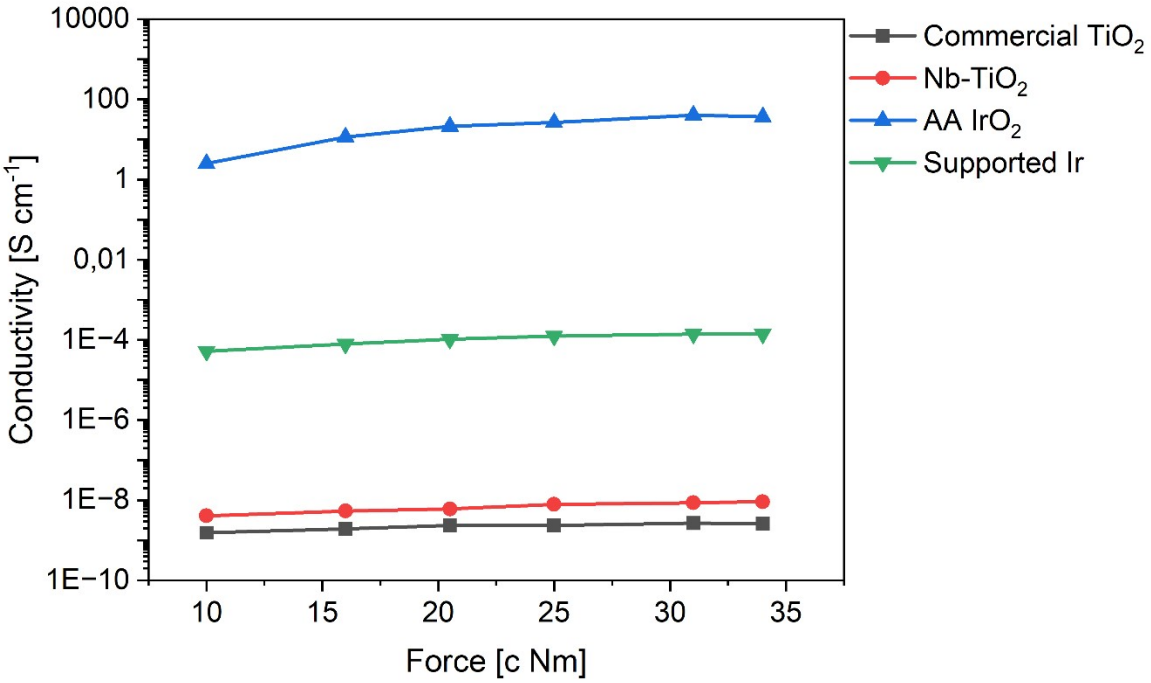

Figure S3. Conductivity values measured as a function of applied force for commercial TiO_2 (black), Nb-TiO_2 (red), AA IrO_2 (blue), and the as-synthesized catalyst (green). While the commercial TiO_2 and AA IrO_2 measurements align with the conductivity ranges reported in literature,[3,4] the synthesized Nb-TiO_2 shows a conductivity similar to undoped TiO_2, which is at least 3 orders of magnitude lower than previously reported values for Nb-TiO_2.[5,6] The as-synthesized supported Ir catalyst exhibits a conductivity at least 5 orders of magnitude lower than typical values for IrO_2 and metallic Ir.[4,7,8] This discrepancy is likely due to poor dispersion of the metal nanoparticles across the support.

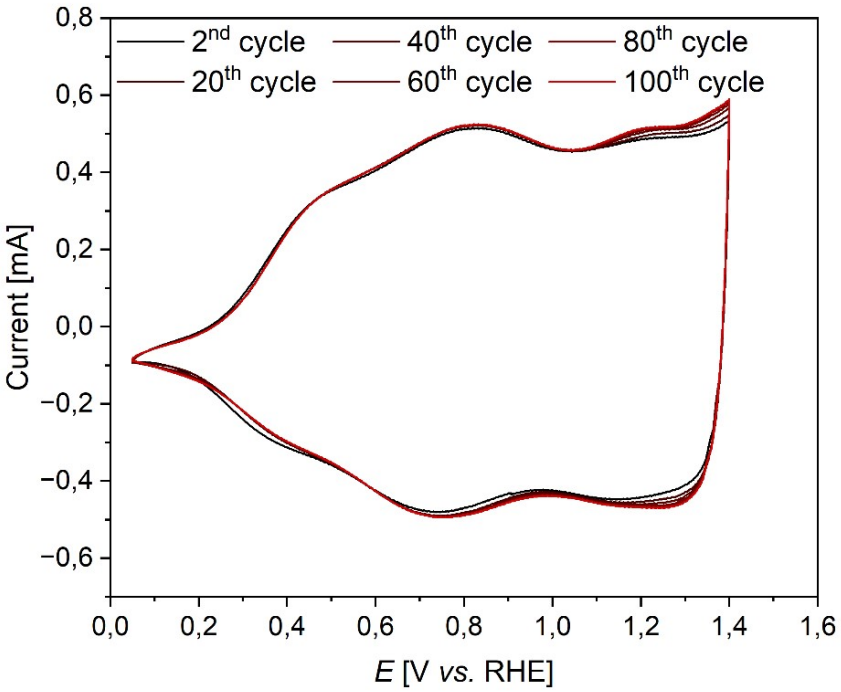

Figure S4. CVs of AA IrO_2 during electrochemical oxidation.

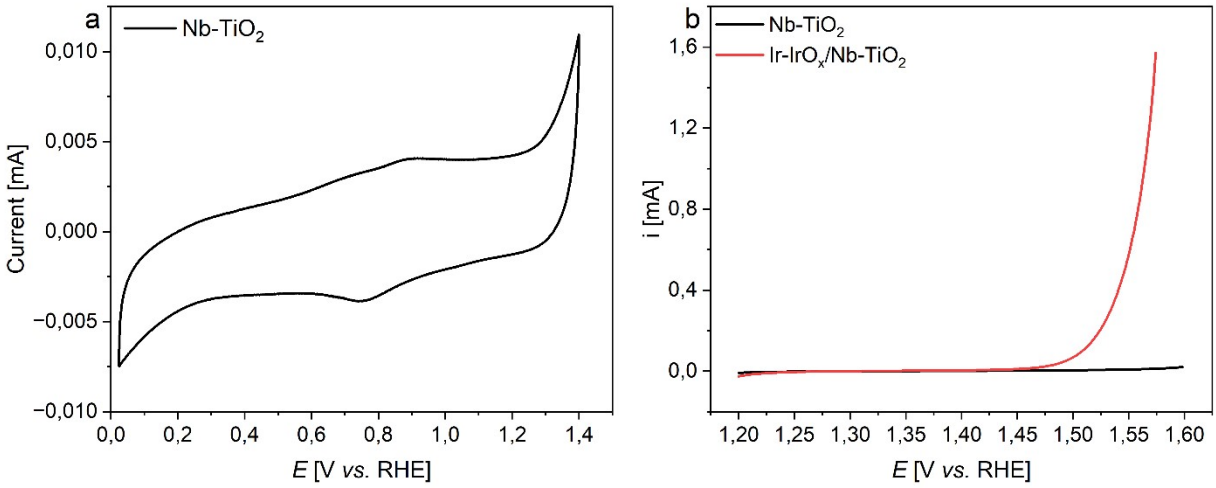

Figure S5. (a) CV of the bare Nb-TiO_2 support. (b) OER activity of the Nb-TiO_2 support (black). The corresponding activity of the supported catalyst (red) is shown for comparison.

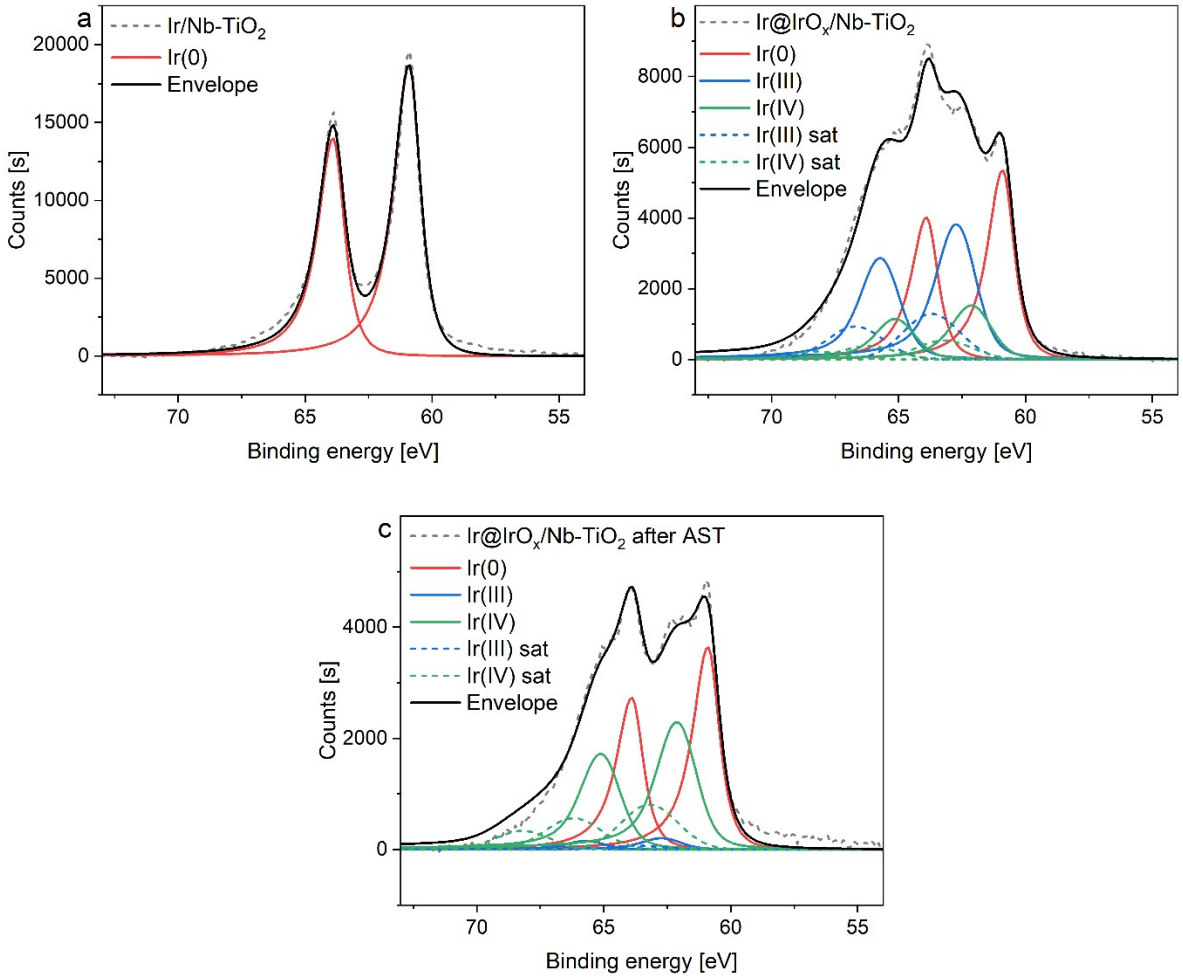

Figure S6. XPS fittings of (a) pristine Ir/Nb–TiO_2, (b) Ir@IrO_x/Nb–TiO_2 after electrochemical oxidation and (c) Ir@IrO_x/Nb–TiO_2 after AST. The proposed fitting in the figures was performed with the binding energy and satellite peak parameters used for oxidized Ir nanoparticles provided by Tan et al.,[9] with the lineshapes for Ir(0), Ir(III) and Ir(IV) from Wagner et al.[10] However, given the presence of multiple species and the resulting challenges in reliably assigning peak positions and shapes, these data should be interpreted with caution.

References

1. Pfeifer, V. *et al.* The electronic structure of iridium oxide electrodes active in water splitting. *Physical Chemistry Chemical Physics* **18**, 2292–2296 (2016).

2. Willinger, E., Massué, C., Schlögl, R. & Willinger, M. G. Identifying Key Structural Features of IrOx Water Splitting Catalysts. *J. Am. Chem. Soc.* **139**, 12093–12101 (2017).

3. Yildiz, A., Lisesivdin, S. B., Kasap, M. & Mardare, D. Electrical properties of TiO2 thin films. *J. Non. Cryst. Solids* **354**, 4944–4947 (2008).

4. Lam, A. *et al.* Structure of Iridium Oxides and Their Oxygen Evolution Electrocatalysis in Acidic Media. *ACS Catal.* 8414–8425 (2025) doi:10.1021/acscatal.5c01659.

5. Liu, Y. *et al.* Niobium-Doped Titania Nanoparticles: Synthesis and Assembly into Mesoporous Films and Electrical Conductivity. *ACS Nano* **4**, 5373–5381 (2010).

6. Furubayashi, Y. *et al.* A transparent metal: Nb-doped anatase TiO2. *Appl. Phys. Lett.* **86**, 1–3 (2005).

7. Technical data for the element Iridium in the Periodic Table. https://periodictable.com/Elements/077/data.html.

8. White, G. K. & Woods, S. B. THERMAL AND ELECTRICAL CONDUCTIVITY OF RHODIUM, IRIDIUM, AND PLATINUM. *Can. J. Phys.* **35**, 248–257 (1957).

9. Tan, X., Shen, J., Semagina, N. & Secanell, M. Decoupling structure-sensitive deactivation mechanisms of Ir/IrOx electrocatalysts toward oxygen evolution reaction. *J. Catal.* **371**, 57–70 (2019).

10. X-ray Photoelectron Spectroscopy (XPS) Reference Pages: Iridium. https://www.xpsfitting.com/2008/10/iridium.html.